JACS
JOURNAL OF THE AMERICAN CHEMICAL SOCIETY

Article

pubs.acs.org/JACS

Molecular Characterization of the Cercosporin Biosynthetic Pathway in the Fungal Plant Pathogen *Cercospora nicotianae*

Adam G. Newman and Craig A. Townsend*

Department of Chemistry, Johns Hopkins University, Baltimore, Maryland 21218, United States

Supporting Information

ABSTRACT: Perylenequinones are a class of photoactivated polyketide mycotoxins produced by fungal plant pathogens that notably produce reactive oxygen species with visible light. The best-studied perylenequinone is cercosporin—a product of the *Cercospora* species. While the cercosporin biosynthetic gene cluster has been described in the tobacco pathogen *Cercospora nicotianae*, little is known of the metabolite's biosynthesis. Furthermore, *in vitro* investigations of the polyketide synthase central to cercosporin biosynthesis identified the naphthopyrone *nor*-toralactone as its direct product—an observation in conflict with published biosynthetic proposals. Here, we present an alternative biosynthetic pathway to cercosporin based on metabolites characterized from a series of biosynthetic gene knockouts. We show that *nor*-toralactone is the key polyketide intermediate and the substrate for the unusual didomain protein CTB3. We demonstrate the unique oxidative cleavage activity of the CTB3 monooxygenase domain *in vitro*. These data advance our understanding of perylenequinone biosynthesis and expand the biochemical repertoire of flavin-dependent monooxygenases.

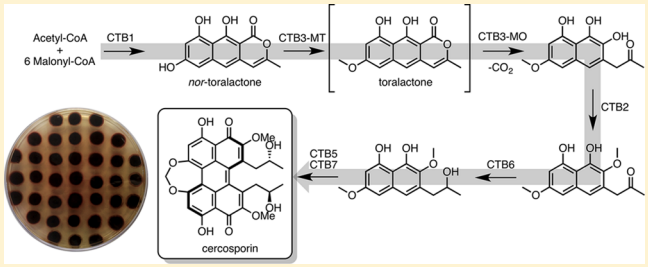

INTRODUCTION

The plant pathogenic *Cercospora* species are a widespread and destructive genus of ascomycetous fungi characterized by their production of the phytotoxin cercosporin (**1**, Figure 1b).[1] Cercosporin belongs to the perylenequinone natural product family. The perylenequinone metabolites share a characteristic core architecture (**2**) that is essential to their toxicity.[2,3] Multiple perylenequinone natural products have been identified from fungal and aphidian sources.[4] Cercosporin was first isolated in 1957 from *Cercospora kikuchii* T. Matsu and Tomoyasu—a fungal pathogen of soybeans.[5,6] Perylenequinone metabolites contain the same highly oxidized conjugated pentacyclic core regardless of varied substituents—primarily at positions C7 and C7′—and are typically C_2-symmetric. Notably, most perylenequinone metabolites are helically chiral, demonstrating a preference for one particular atropisomer despite their conjugated, sp^2-hybridized carbon core.[7−9] Steric clashes between substituents in the mature dimeric metabolites account for the observed helical chirality. The biosynthetic origin of this property is unknown.

Cercosporin—like all perylenequinone metabolites—functions as a photosensitizing agent.[10] Upon absorption of visible light, cercosporin facilitates remarkably efficient transfer of this energy to O_2 (quantum yield 0.81[11]), leading to the production of the potent reactive oxygen species (ROS) singlet oxygen ($^1O_2$) and superoxide radical ($O_2^{\bullet-}$). These ROS cause indiscriminate damage to a variety of cellular targets including cell membranes, nucleic acids, proteins, and lipids.[12−14] Peroxidation of the cell membrane is particularly pernicious and is the primary mode of toxicity, causing ion leakage from the host organism.[12,13] A direct cellular target of cercosporin has not been found but it is believed that its toxicity is entirely attributed to indiscriminant damage by ROS. As a result, cercosporin exerts broad toxicity to bacteria, fungi, and mice.[15−17] Production of cercosporin by *Cercospora nicotianae*—a fungal pathogen of tobacco—is crucial to the fungus's pathogenicity and is concomitant with lesion formation on tobacco leaves.[18−20] Multiple putative resistance mechanisms have been proposed in *C. nicotianae*, but the primary mode of resistance is through reversible reduction of the perylenequinone moiety to dihydrocercosporin (**3**)—a species with little photosensitizing capacity. Dihydrocercopsorin is oxidized to cercosporin spontaneously upon export from the fungus, restoring its photoactivated toxicity.[21−23]

Cercosporin was classified early on as a polyketide natural product and bore the characteristic alternating polyketide labeling pattern from acetyl and malonyl building blocks.[24] Eventually a gene from *C. nicotianae* encoding a fungal polyketide synthase—dubbed CTB1 (cercosporin toxin biosynthesis 1)—was identified through restriction enzyme-mediated integration mutagenesis.[18] CTB1 is absolutely necessary for cercosporin production and bears all the hallmarks of an iterative, nonreducing polyketide synthase (NR-PKS).[25] Using CTB1 as a benchmark, the complete cercosporin biosynthetic gene cluster from *C. nicotianae* was determined (Figure 1a, Table 1).[26] The cluster comprises eight genes, six of which are believed to be responsible for cercosporin assembly (CTB1, 2,

Received: January 18, 2016
Published: March 3, 2016

DOI: 10.1021/jacs.6b00633
J. Am. Chem. Soc. 2016, 138, 4219−4228

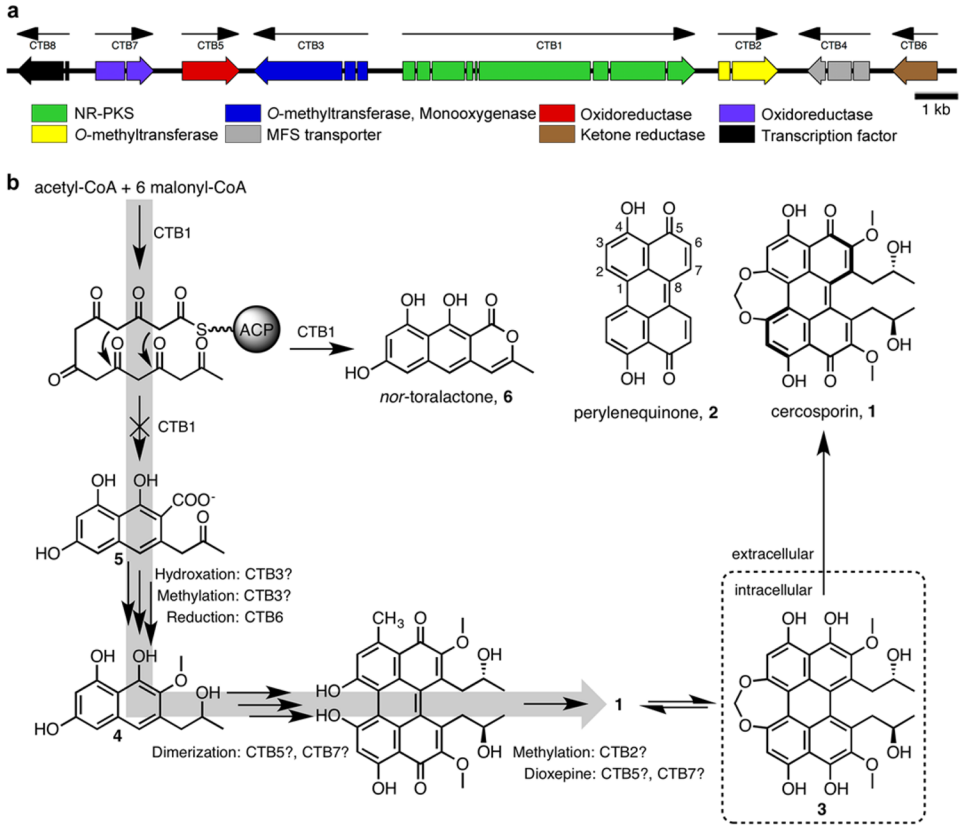

Figure 1. Currently proposed cercosporin biosynthetic pathway. (a) The cercosporin toxin biosynthetic (CTB) gene cluster has been identified in *C. nicotianae*. (b) The proposed cercosporin biosynthesis hinges upon the formation of carboxylic acid **5** by the NR-PKS CTB1. The direct product of CTB1 is *nor*-toralactone (**6**), precluding the proposed biosynthetic scheme.

Table 1. Cercosporin Biosynthetic Gene Cluster from *C. nicotianae*

gene	accession number	length (bp)	intron	amino acids	domains and motifs	InterPro annotation	predicted function
CTB1	AY649543	7036	8	2196	PKS β-ketoacyl synthase	IPR020841	*nor*-toralactone synthase
					PKS acyl transferase	IPR020801	
					Polyketide product template domain	IPR030918	
					Acyl carrier protein-like	IPR009081	
					PKS thioesterase domain	IPR020802	
CTB2	DQ991505	1439	1	461	O-methyltransferase, family 2	IPR001077	*O*-methyltransferase
CTB3	DQ355149	2734	2	871	O-methyltransferase, family 2	IPR001077	*O*-methyltransferase FAD-dependent monooxygenase
					Monooxygenase, FAD-binding	IPR002938	
CTB4	DQ991506	1696	3	512	Major facilitator superfamily domain	IPR020846	MFS transporter
CTB5	DQ991507	1380	0	459	FAD linked oxidase, N-terminal	IPR006094	FAD-dependent oxidoreductase
CTB6	DQ991508	1074	0	357	NAD(P)-binding domain	IPR016040	NAD(P)H-dependent ketone reductase
CTB7	DQ991509	1401	1	450	Monooxygenase, FAD-binding	IPR002938	FAD-dependent monooxygenase
CTB8	DQ991510	1245	1	397	Zn(2)-C6 fungal-type DNA binding domain	IPR001138	Transcription factor
					Aflatoxin regulatory protein	IPR013700	

3, 5, 6, and 7).[18,20,26,27] The zinc finger transcription factor CTB8 coregulates expression of the cluster,[26] while the major facilitator superfamily (MFS) transporter CTB4 exports the final metabolite.[19] In addition to the identified gene cluster, the Zn(II)Cys_6 transcription factor CRG1 is implicated in both cercosporin production and resistance.[28−30] The Zn(II)Cys_6 family of transcription factors is unique to fungi that regulate diverse cellular processes.[31] Regulation by CRG1 is complex and poorly understood; however, its expression is implicated in regulation of chemical detoxification, multidrug membrane transport, and antioxidant biosynthesis pathways.[30] Cercosporin production is completely dependent upon exposure to light, and *C. kikuchii* grown in the dark will not accumulate cercosporin.[32] The regulatory mechanism governing light dependence is unknown.

On the basis of individual homologies of the *C. nicotianae* gene cluster and retrobiosynthetic analysis, Chen and coworkers proposed a biosynthetic pathway for cercosporin (Figure 1b).[26] This proposal hinges upon the metabolite's C_2-symmetry and the authors argued that dimerization of two

DOI: 10.1021/jacs.6b00633
J. Am. Chem. Soc. 2016, 138, 4219−4228

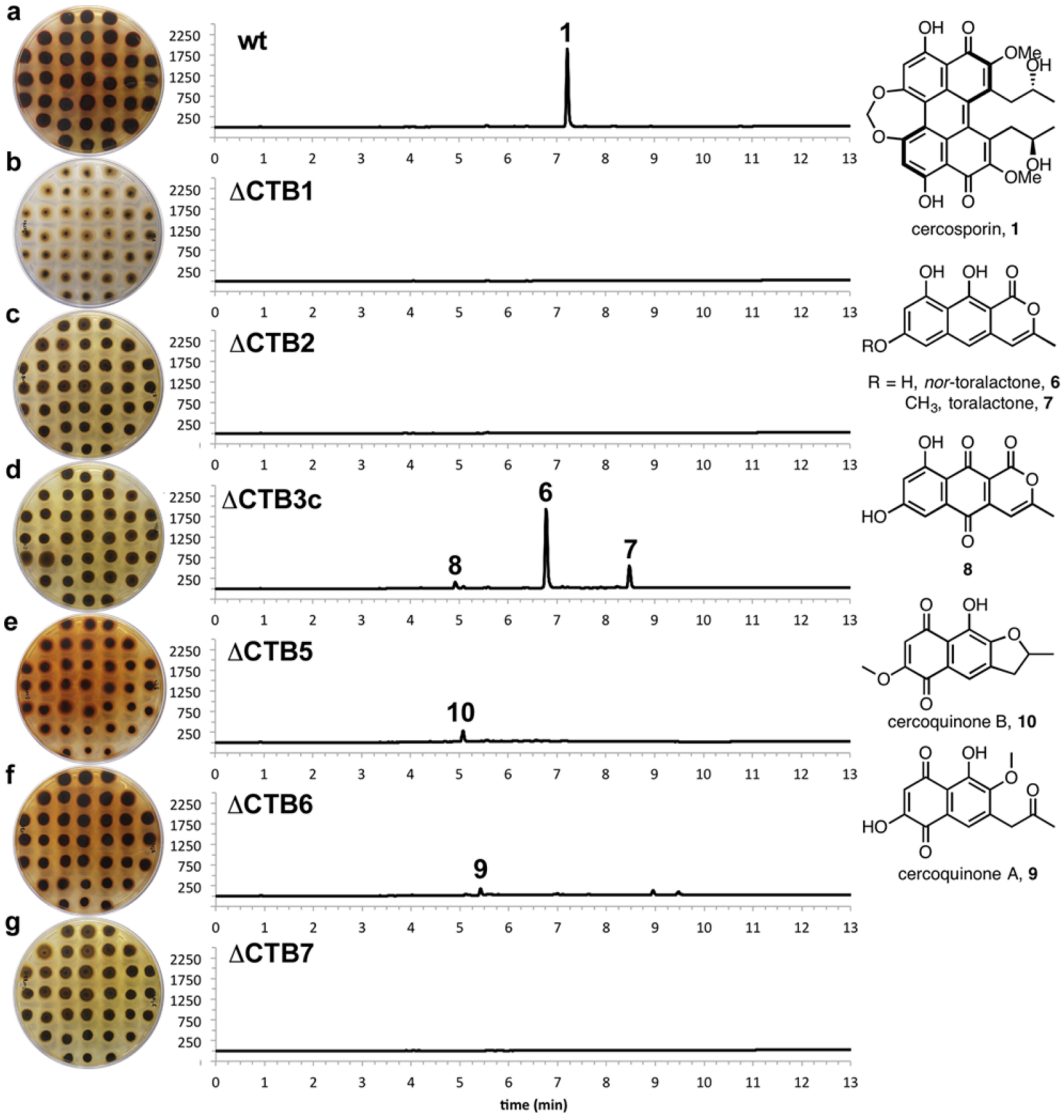

Figure 2. Metabolic profiles of CTB gene cluster mutant strains. Chromatograms at 250 nm of extracted metabolite profiles for (a) wild-type, (b) ΔCTB1, (c) ΔCTB2, (d) ΔCTB3c, (e) ΔCTB5, (f) ΔCTB6, and (g) ΔCTB7 strains displayed along with images of the mycelia for each strain. The metabolites were prepared at a concentration of 10 cm^2 colony surface area per mL in methanol. Identified cercosporin intermediate metabolites are displayed.

identical aromatic intermediates **4** would lead to the perylenequinone core. They postulated that CTB1 produces carboxylic acid **5** from which the aromatic intermediate **4** is derived. While this biogenesis appears reasonable and accounts for the putative activity of all the biosynthetic gene cluster members, it is nevertheless likely incorrect. Using an enzyme-deconstruction approach, we previously characterized the *in vitro* activity of CTB1.[25] Unexpectedly, the naphthopyrone *nor*-toralactone (**6**) is the unambiguous *in vitro* product of CTB1 (Figure 1b). The identification of this intermediate is problematic, as there is no clear member of the gene cluster that could presumably open the pyrone moiety—an event that must occur to access the perylenequinone core architecture. We present an alternative biosynthetic pathway bolstered by metabolites accumulated in pathway-interrupted *C. nicotianae* knockouts. Furthermore, we characterize the *in vitro* activity of CTB3—an unusual didomain protein containing *O*-methyltransferase and flavin-dependent monooxygenase domains—and demonstrate its role in toralactone formation—an *O*-methylated congener of *nor*-toralactone—and subsequent pyrone opening.

RESULTS

Chemical Identification of Intermediates. *C. nicotianae* has been previously cultivated in liquid potato dextrose broth (PDB) and on solid potato dextrose agar (PDA). While functional cercosporin biosynthetic gene knockout strains of *C. nicotianae* grew in PDB, reproducible metabolite profiles could not be obtained. Therefore, metabolites were isolated from cultures grown on PDA under constant light, which provided reproducible metabolite profiles. Cultures of wild-type *C. nicotianae* resulted in a clean metabolic profile with the red-pigmented cercosporin (**1**) as the principal product (Figure 2a). Cercosporin was absent in the HPLC profiles of all functional cercosporin biosynthetic gene knockout strains. As expected, secondary metabolite accumulation was missing in the ΔCTB1 mutant—the knockout mutant of the central NR-PKS of cercosporin biosynthesis (Figure 2b).

DOI: 10.1021/jacs.6b00633
J. Am. Chem. Soc. 2016, 138, 4219−4228

The structures of the major accumulated metabolites from *C. nicotianae* CTB gene cluster knockout strains were elucidated by characteristic UV spectra, exact masses, mass fragmentation patterns, and where possible NMR spectra. We identified the previously characterized naphthopyrones *nor*-toralactone (**6**) and toralactone (**7**) both as metabolites of the ΔCTB3c mutant (Figure 2d). Also accumulated in the ΔCTB3c mutant was the oxidation product of *nor*-toralactone, naphthoquinone **8**. Two previously unobserved naphthoquinones were isolated from the ΔCTB6 and ΔCTB5 mutants, which we called cercoquinone A (**9**) and cercoquinone B (**10**), respectively (Figure 2f,e). No major compounds were observed in the extracted metabolite profiles for the ΔCTB2 and ΔCTB7 mutants (Figure 2c,g). The profiles for each of these mutants were similar to that of the ΔCTB1 mutant. Proposed structural assignments for new compounds cercoquinones A and B are supported by their ^{1}H NMR spectra, HRMS, mass fragmentation patterns and UV spectra (see Supporting Information).

Phenotypic Analysis of Gene Knockout Strains. The mycelia of wild-type *C. nicotianae* were blood red in color, with pigmentation occurring at about 4 days after inoculation (Figure 2a). The pigmented metabolites were primarily concentrated in the mycelia with a small amount exported into the agar surrounding individual colonies. The mycelia of each knockout strain displayed a different pigmentation from wild-type *C. nicotianae*, with pigmentation similarly occurring at about 4 days after inoculation. The ΔCTB1 mutant did not display any pigmentation (Figure 2b). The ΔCTB3c mutant adopted a dark yellow-brown coloration, with slight export of pigmented metabolites into the agar (Figure 2d). The mycelia of both ΔCTB6 and ΔCTB5 mutants turned a dark orange-red with significant export of colored compounds into the agar (Figure 2f,e). Although they did not accumulate any observed extractable secondary metabolite observed by HPLC, the mycelia of the ΔCTB2 and ΔCTB7 mutants both adopted a yellow-brown color with some export of pigmented compounds into the agar (Figure 2c,g).

In addition to the pigmentation phenotypes, the average colony diameter for each individual strain was distinctive after 7 days of growth (Figure 3b). The average colony diameters for the wild-type, ΔCTB3c, and ΔCTB6 strains were the smallest at 15.5 ± 0.8, 15.7 ± 1.1, and 15.9 ± 1.0 mm (average ± standard deviation, n = 37). The average colony diameter for the ΔCTB5 mutant was of intermediate size at 17.1 ± 1.1 mm, while the average colony diameters for the ΔCTB1, ΔCTB2, and ΔCTB7 mutants were the largest at 20.8 ± 1.3, 19.2 ± 1.4, and 18.7 ± 1.8 mm, respectively. The average colony diameter showed an inverse correlation with small molecule accumulation; the strains with identifiable cercosporin metabolites (wild-type, ΔCTB3c, ΔCTB6, and ΔCTB5) displayed smaller colony diameters, while the strains without identifiable extractable intermediates (ΔCTB1, ΔCTB2, and ΔCTB7) displayed larger colony diameters.

Cercosporin Complementation Assay. To test whether accumulated metabolites represented on-pathway intermediates, we conducted a complementation assay in which pairs of CTB gene cluster knockout strains were grown adjacent to one another. Cercosporin biosynthetic complementation was indicated by red pigmentation at the colony−colony interface. The only pair that could successfully complement cercosporin biosynthesis was the ΔCTB1 and ΔCTB3c mutant pair (Figure 3a). Clear complementation was observed between 4 and 5 days after inoculation between colonies spotted approximately 0.5 cm apart. Pigmentation was isolated to the ΔCTB1 mutant with no clear accumulation of cercosporin in the ΔCTB3c mutant. We attempted to detect cercosporin extracted from agar plugs of the colony−colony interface using a previously described spectrophotometric assay;[33] however, the amount of accumulated cercosporin was below the detection limit. No other mutant pair showed clear cercosporin complementation (Figure S3, Supporting Information).

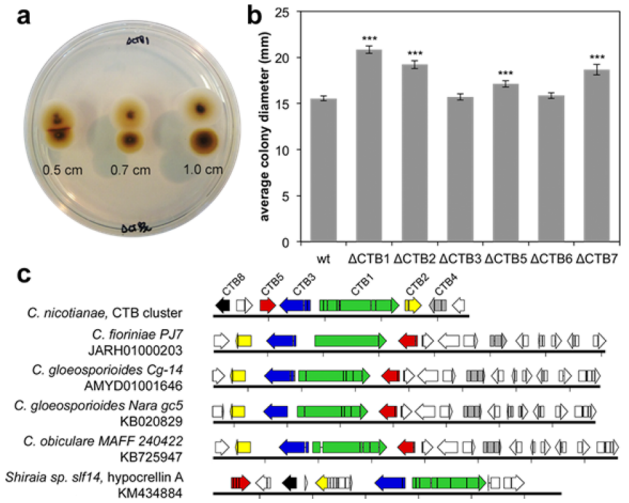

Figure 3. Phenotypic and genetic analysis of the CTB cluster. (a) Cercosporin biosynthesis was complemented at the colony−colony interface of the ΔCTB1/ΔCTB3c mutant pair (top/bottom, respectively). The numbers indicate the distance that colonies were inoculated apart from one another in cm. (b) Average colony diameters of CTB disruption mutants are displayed (n = 37). Error bars represent the 95% confidence interval. Stars indicate statistically significant difference from wild-type (p < 0.01). (c) Comparison of gene clusters similar to the CTB gene cluster of *C. nicotianae* (top).

Genetic Analysis of the Cercosporin Gene Cluster. The antiSMASH algorithm was used to identify gene clusters homologous to the CTB gene cluster.[34] The top five sequences all came from fungal plant pathogens (Figure 3c). Of these sequences, only one was associated with a known natural product, the hypocrellin A biosynthetic cluster from *Shiraia* sp. slf14 responsible for the formation of the perylenequinone hypocrellin A (**13**).[35] Five homologous CTB genes were shared among all identified clusters: homologues of CTB1, 3, 2, 5, and 4. The CTB1 homologues contained the canonical NR-PKS domain architecture as determined by a BLASTp search. All of the homologues of CTB3 displayed the same unique didomain architecture with a predicted *N*-terminal *O*-methyltransferase and a *C*-terminal flavin-dependent monooxygenase.

***In Vitro* Analysis of CTB3 Activity.** Initially deducing that it followed CTB1 on the cercosporin pathway, we investigated the *in vitro* activity of CTB3 toward *nor*-toralactone—the *in vitro* product of CTB1. Because of its unique didomain architecture, we dissected CTB3 into its constituent domains—the *N*-terminal *O*-methyltransferase (CTB3-MT) and the *C*-terminal flavin-dependent monooxygenase (CTB3-MO)—for ease of expression and to investigate the activity of each domain individually (Figure S1, Supporting Information). Both CTB3 and CTB3-MO were purified as *holo* enzymes with the FAD cofactor bound to the proteins. The presence of FAD was confirmed by HPLC and spectrophotometric analysis (Figure S2, Supporting Information). Cosubstrates SAM and NADH

DOI: 10.1021/jacs.6b00633
J. Am. Chem. Soc. 2016, 138, 4219−4228

were included in reactions of CTB3 as needed. SAM served as the methyl donor for CTB3-MT and NADH served as the reductant for CTB3-MO—transferring a hydride equivalent to FAD at the initiation of a catalytic cycle.

In vitro reactions were conducted with both *nor*-toralactone (**6**) and toralactone (**7**) as substrates. Initial reactions containing 10 μM CTB3 clearly processed these substrates; however, the product profiles were ambiguous. Furthermore, the CTB3-MO domain processed both potential substrates with *nor*-toralactone being converted to a host of products. While these species were not fully characterized, MS and UV data were indicative of perylenequinone-like products with the clear loss of a single carbon. In order to simplify analysis of these enzymatic reactions, significant effort went into optimizing the experimental conditions. We found that lower protein concentrations (1 μM) and simplified sample preparation (filtration only before HPLC analysis) were necessary for reproducible and robust analysis.

Reactions of CTB3-MT showed turnover of *nor*-toralactone to toralactone (Figure 4a). Similarly, reactions containing a low concentration of protein (0.1 μM) showed partial methylation of *nor*-toralactone to toralactone. Together, these results indicated that toralactone served as an intermediate of the CTB3 catalytic cycle and was the true substrate for the CTB3-MO domain despite its apparent activity toward *nor*-toralactone. Postulating that the programming of the catalytic cycle between the MT and MO domains was in part kinetically controlled, we conducted reactions that were allowed to proceed for 60 min before quenching—significantly longer than the 7−10 min reactions initially employed. Reactions of the CTB3-MO domain with toralactone serving as the substrate resulted in turnover to *o*-naphthoquinone **12**—cercoquinone C (Figure 4b). Cercoquinone C was also observed in reactions of deconstructed CTB3 with *nor*-toralactone as the substrate—albeit with a coterie of other uncharacterized products (Figure 4c). These additional products were absent in reactions with toralactone. Additionally, toralactone is an observed intermediate of this reaction along with the off-pathway oxidation product, naphthoquinone **8**.

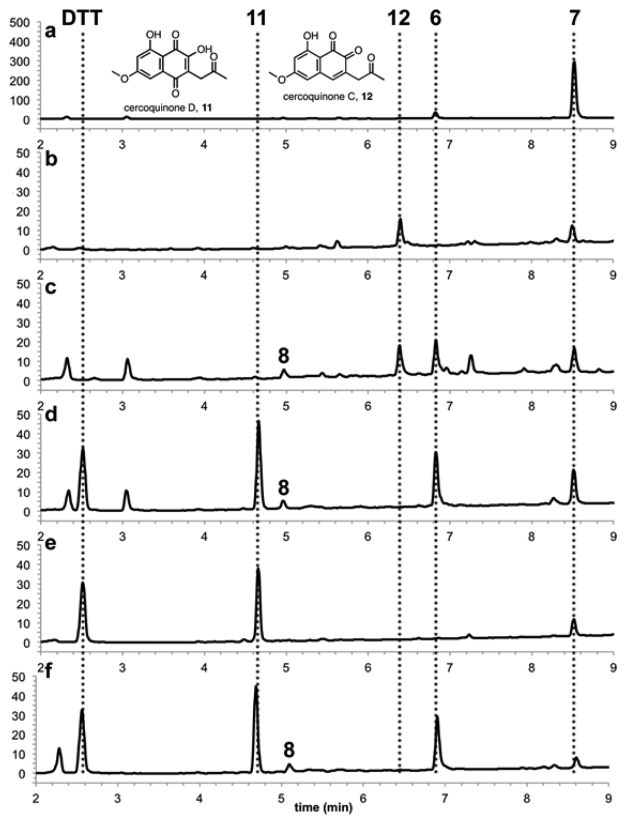

Figure 4. Product profiles of *in vitro* reactions of CTB3. The 280 nm chromatograms of the following reactions are displayed: (a) CTB3-MT with *nor*-toralactone, (b) CTB3-MO with toralactone, (c) CTB3-MT and CTB3-MO with *nor*-toralactone, (d) CTB3-MT and CTB3-MO with *nor*-toralactone under reductive conditions, (e) CTB3-MO with toralactone under reductive conditions, and (f) CTB3 with *nor*-toralactone under reductive conditions. Peaks for *nor*-toralactone (**6**) and toralactone (**7**) are indicated along with peaks for products cercoquinone C (**12**) and cercoquinone D (**11**). Peaks for DTT and other cosubstrates are observed, as applicable.

The formation of cercoquinone C was unexpected. Presumably, this product is formed through its dihydroquinone (**14**) even though that species was not directly observed. Assuming that oxidation was spontaneous, we postulated that conducting *in vitro* reactions under reductive conditions could have prevented the presumptive oxidation. Reactions under reductive conditions (1 mM DTT) resulted in the formation of a new *p*-naphthoquinone **11**—cercoquinone D (Figure 4d−f). Cercoquinone D was only observed when DTT was present. It was observed in either reactions of combined CTB3-MT and CTB3-MO or intact CTB3 with *nor*-toralactone and reactions of the CTB3-MO domain with toralactone. Time-course experiments showed that the appearance of either cercoquinone C under nonreductive conditions and cercoquinone D under reductive conditions was coincident with the consumption of toralactone by CTB3-MO and no other intermediates were detectable. Exhaustive attempts to capture the putative intermediate **14** through methylation by CTB2, an *O*-methyltransferase, were unsuccessful. Reactions contained either CTB2 and CTB3 or CTB2 and CTB3-MO or CTB2 and CTB3-MT, with *nor*-toralactone or toralactone, respectively, serving as a substrate. As expected, CTB2 was unsuccessful at methylating *nor*-toralactone. Furthermore, it did not alter cercoquinones C and D formation by CTB3, as previously observed (Figure S4, Supporting Information).

Structural assignments of cercoquinones C and D were supported by HRMS, mass fragmentation, and UV spectral data. Insufficient amounts of material made structural analysis by NMR for these products unfeasible. Structural analogues of both cercoquinones C and D containing the same quinone cores display similar UV spectra.[36] The fragmentation data were highly characteristic (Schemes S2 and S3, Supporting Information). As with cercoquinones A and B, fragmentation ions were observed that comport with the naphthoquinone core. It should be noted that 1,2-naphthoquinones and 1,4-naphthoquinones each fragment in distinct ways.[37] Additionally, substituents at the C3 position—the 2-oxopropyl moieties in cercoquinones C and D—can influence the fragmentation of the quinone ring.[37−39] Mass fragmentation results for cercoquinones C and D are presented in detail in the Supporting Information.

DISCUSSION

The results presented herein resolve the uncertainties about cercosporin biosynthesis and point to a common biosynthetic pathway for the perylenequinone natural products.[25,26] We propose a revised biosynthetic scheme for cercosporin based upon the accumulated metabolites of functional biosynthetic

DOI: 10.1021/jacs.6b00633
J. Am. Chem. Soc. 2016, 138, 4219−4228

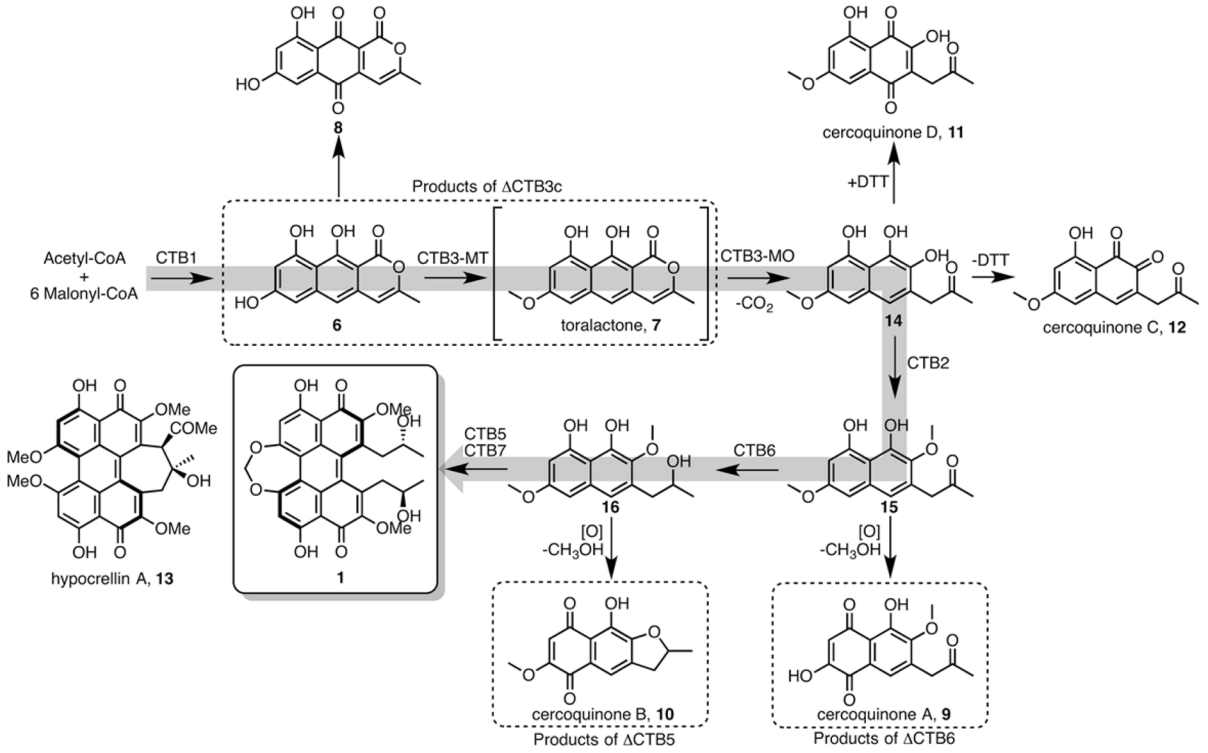

Figure 5. Proposed cercosporin biosynthetic pathway. On the strength of observed pathway intermediates, *in vitro* chemistry, phenotypic, genetic, and pairwise complementation a revised biosynthetic scheme for cercosporin is presented.

Scheme 1. Proposed Formation of Cercoquinone A[a]

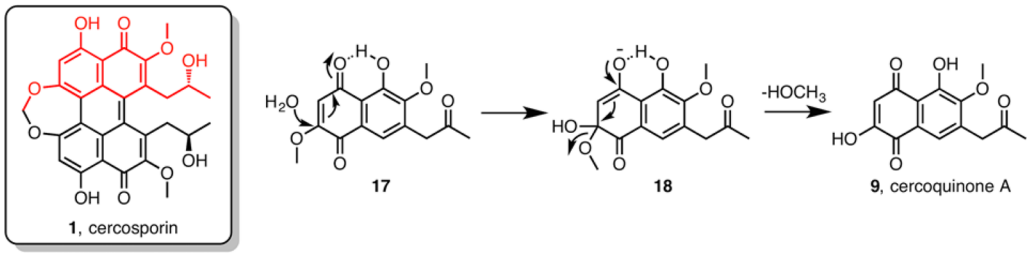

[a]Two mechanisms were considered. Addition of water followed by elimination of methanol (pictured) or enzymatic demethylation. Cercosporin is shown with a monomeric unit shown in red. CTB7 is postulated to form the dioxepine ring, a transformation that would require the elimination of a methyl group at the position of demethylation in cercoquinone A.

gene knockout strains (Figure 5). First, CTB1 acts according to its established *in vitro* chemistry producing *nor*-toralactone (**6**).[25] The bifunctional enzyme CTB3 methylates *nor*-toralactone to toralactone (**7**) before conducting an unusual oxidative aromatic ring opening producing metabolite **14**. The *O*-methyltransferase CTB2 is proposed to methylate the nascent OH-6 of intermediate **14**—blocking further oxidation at this site and yielding compound **15**—before the reductase CTB6 reduces the 2-oxopropyl ketone at position C7, giving naphthalene **16**. CTB5 is thought to be responsible for homodimerization of intermediate **16** with CTB7 installing the dioxepine moiety, finally producing cercosporin (**1**).

We suggest that several of the accumulated metabolites correspond to oxidation products of true on-pathway intermediates. The metabolites cercoquinone A (**9**) and cercoquinone B (**10**) from the ΔCTB6 and ΔCTB5 mutants, respectively, fall into this category. Both quinone products derive from the oxidation of electron-rich naphthalene derivatives. The oxidation of electron-rich aromatic metabolites is common and spontaneous—often leading to stabilized products.[40] ^{1}H NMR and mass fragmentation data support these structural assignments, especially with respect to the sites of oxidation and methylation. Indeed, the observed fragmentation ions agreed with established fragmentation mechanisms for naphthoquinone products.[37−39] The inability of either ΔCTB6 or ΔCTB5 mutants to complement cercosporin activity as secretor-converter pairs bolsters the argument that cercoquinones A and B are rapidly formed off-pathway byproducts by spontaneous oxidation.

Interestingly, cercoquinone A displays the loss of a methyl group installed earlier through the activity of the *O*-methyltransferase domain of CTB3. The loss of the methyl at this position is, however, unambiguous given the metabolite's characteristic mass fragmentation pattern; in particular, the retention of the methoxyl in both a ring contraction carbocation and a ring-opened oxonium ion confirms its structural assignment. We envision two possible scenarios that could account for the elimination of this moiety (Scheme 1). In

DOI: 10.1021/jacs.6b00633
J. Am. Chem. Soc. 2016, 138, 4219−4228

Scheme 2. Proposed Mechanism for CTB3 Flavin-Dependent Monooxygenase Domain[a]

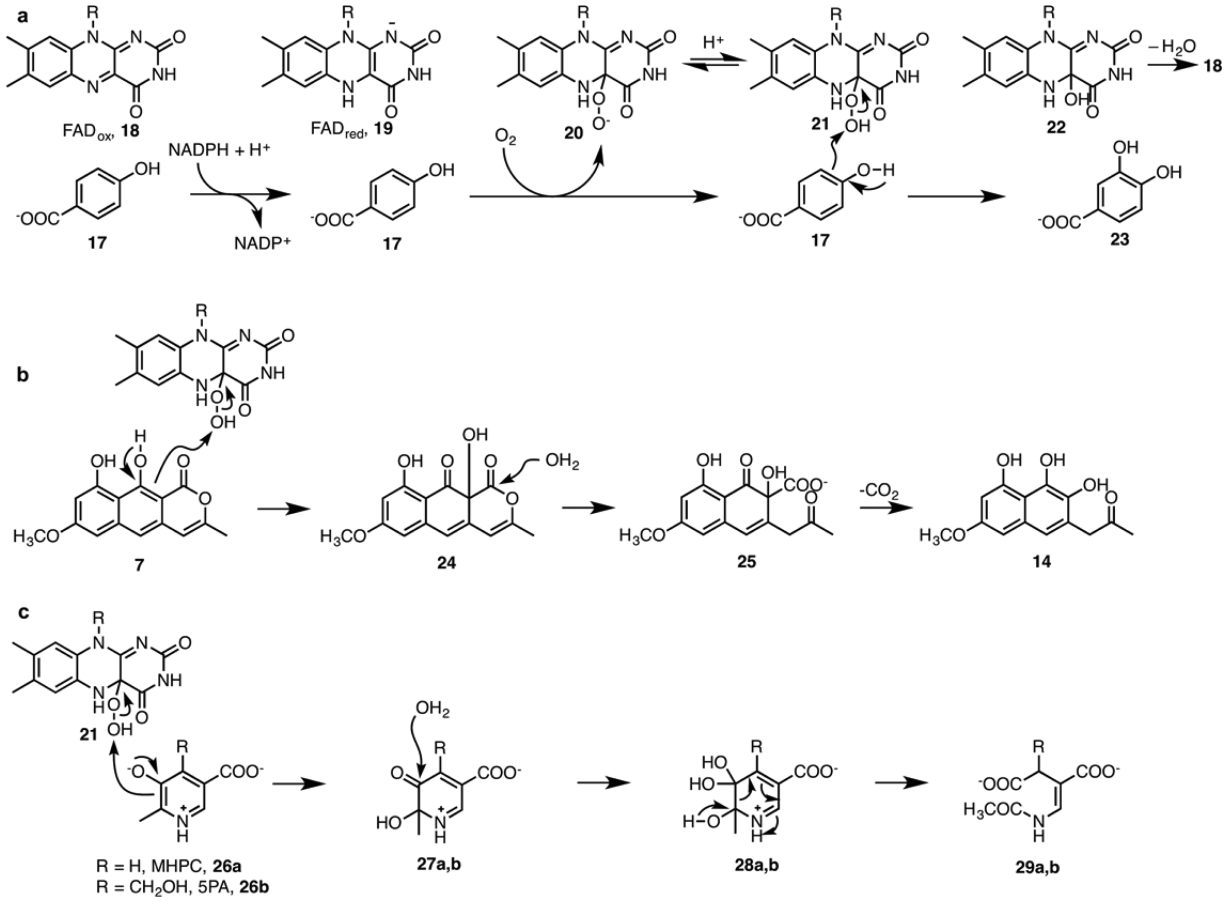

[a](a) General mechanism of *p*-hydroxybenzoate (**17**) hydroxylase family members. (b) Proposed mechanism for CTB3 catalyzed oxidative aromatic ring cleavage of toralactone (**7**). (c) Mechanism of MHPCO and 5PAO oxidative aromatic ring cleavage.

the first possibility, it is simply eliminated as methanol following oxidation and addition of water to the *p*-quinone activated by internal hydrogen bonding. In the second possibility, the methyl position is removed enzymatically. The methoxy at this position is eventually incorporated into the dioxepine functionality of the final product we believe through the activity of CTB7. While the mechanism of this transformation is unknown, by analogy to studies of methylenedioxy formations,[41,42] it would likely involve oxidative loss. Given the structural similarity of cercoquinone A to the monomeric unit of cercosporin, we suggest that CTB7 could accept this metabolite as an alternative substrate and catalyze the elimination of the methyl in question.

The absence of any extractable cercosporin pathway metabolites in the ΔCTB2 and ΔCTB7 mutants is notable given that they are absolutely necessary to sustain cercosporin biosynthesis. Naphthoquinone secondary metabolites in fungi have been shown to inhibit fungal growth.[43] Both ΔCTB2 and ΔCTB7 mutant strains have more robust growth than either wild-type or mutant strains that accumulate significant amounts of naphthoquinone byproducts. Despite their limited metabolic profiles, both ΔCTB2 and ΔCTB7 mutant strains appear pigmented while the ΔCTB1 mutant strain is colorless. The putative cercosporin pathway intermediates produced in these mutant strains would likely be electron-rich, hydroxylated naphthalene analogues similar to the components of melanin.[44] Melanin—a crucial biological pigment—is produced in fungi by the polymerization of polyketide-derived 1,8-dihydroxynaphthalene monomers. It is a critical metabolite in plant pathogens as it provides mechanical strength to cellular structures responsible for host invasion.[45] Furthermore, melanin is highly insoluble and would not contribute to the extracted metabolite profiles analyzed in the current study. Together, the data suggest that the metabolites of the ΔCTB2 and ΔCTB7 mutants are likely captured by a melanin-like self-polymerization pathway resulting in incorporation into insoluble, pigmented polymers.

As has been shown previously, the *in vitro* product of CTB1, an NR-PKS, is naphthopyrone *nor*-toralactone (**6**).[25] The evolution of *nor*-toralactone by the NR-PKS presents an immediate problem. In order to synthesize cercosporin from *nor*-toralactone, the pyrone ring must be opened; however, there is no apparent enzyme in the CTB cluster that could carry out this transformation through conventional lactonase-like hydrolysis—the common pathway for this type of reaction.[46] The accumulation of *nor*-toralactone in the ΔCTB3c mutant simultaneously confirms the importance of this metabolite while implicating a potential candidate in CTB3 for pyrone ring opening. Furthermore, the successful complementation of cercosporin biosynthesis in the ΔCTB1/ΔCTB3c mutant pair corroborates the view that *nor*-toralactone is an on-pathway intermediate.

CTB3 is an unusual didomain enzyme with an *O*-methyltransferase domain and a flavin-dependent monooxyge-

DOI: 10.1021/jacs.6b00633
J. Am. Chem. Soc. 2016, 138, 4219−4228

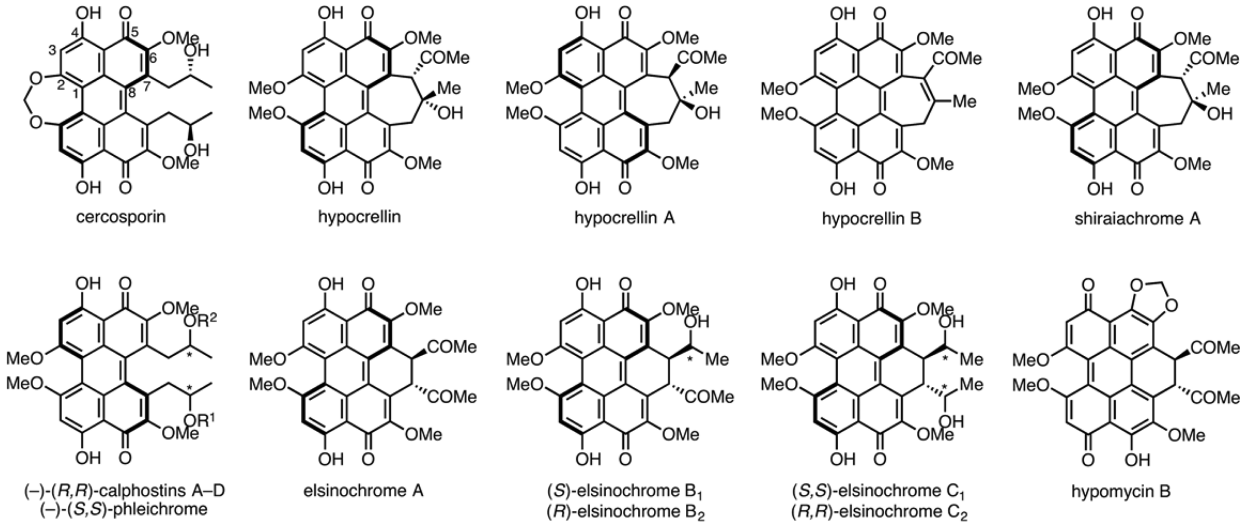

Figure 6. Structures of known fungal perylenequinone natural products. Common architectural features are observed in the family. The occurrence of methyoxy at 2, 2′ and 6, 6′ positions are invariable. As is the 2-oxypropyl derivatives at 7, 7′. The formation of the perylenequinone core also appears to be conserved.

nase domain. The *in vitro* enzymatic reactions presented herein confirm that both domains work in tandem to transform the polyketide product *nor*-toralactone to the on-pathway naphthalene analogue **14**. Although naphthalene **14** is not directly observed, it is the implied shared precursor to both cercoquinone C (**12**) and cercoquinone D (**11**) whose structures are secured by characteristic mass fragments for both *ortho*- and *para*-quinones that confirm the positions of oxidation (Schemes S2 and S3, Supporting Information).

The direct methylation of *nor*-toralactone to toralactone by CTB3-MT, as well as the appearance of toralactone in reactions of CTB3 with *nor*-toralactone are strong indicators that toralactone is a true intermediate of the CTB3 catalytic cycle. Furthermore, its appearance in the metabolite profile of the ΔCTB3c mutant suggests its biosynthetic importance. The ΔCTB3c mutant strain was produced by inserting the knockout cassette into the 3′-terminus of the CTB3 gene corresponding to the CTB3-MO domain. The sequence of the CTB3-MT domain is largely unaltered suggesting the possibility of a functional *O*-methyltransferase. We suspect that the ΔCTB3c mutant strain could retain some endogenous CTB3-MT activity resulting in the partial methylation of *nor*-toralactone in the disruption mutant strain. Alternatively, another *O*-methyltransferase could conceivably convert *nor*-toralactone to toralactone *in vivo*; however, this hypothetical *O*-methyltransferase could not be CTB2—the only other methyltransferase in the CTB cluster as it is incapable of this transformation *in vitro*.

The CTB3-MO domain shares strong primary sequence homology to the canonical *p*-hydroxybenzoate (**17**) hydrolase family of flavin-dependent monooxygenases.[47] This is a well-studied family of enzymes with a shared catalytic mechanism and preference for electron-rich aromatic substrates. They are responsible for the hydroxylation of simple phenolic systems with a preference for the *ortho* and *para* positions. The reaction cycle proceeds in two halves: reductive and oxidative (Scheme 2a).[48] The reductive half cycle is initiated with the formation of a ternary complex of enzyme containing oxidized FAD (FAD_{ox}, **18**), NAD(P)H, and substrate. Upon formation of the ternary complex, rapid reduction of FAD by NAD(P)H occurs (FAD_{red}, **19**). Reduction is contingent on substrate binding or in some cases analogues of the native substrate. $NAD(P)^+$ dissociation occurs at a rate similar to that of reduction. The resulting reduced enzyme and substrate complex has significant kinetic stability. In the oxidative half cycle, oxygen reacts with FAD_{red}, forming the characteristic flavin-C4a-hydroperoxide reactive intermediate (**21**). The deprotonated flavin-C4a-peroxy species (**20**) has never been observed in these enzymes. Hydroxylation of the substrate occurs through electrophilic aromatic substitution resulting in an enzyme-bound product and flavin-C4a-hydroxide (**22**) complex. Water is eliminated from the flavin species resulting in FAD_{ox} and the product is finally released.

We argue that a directly analogous mechanism is at play in the CTB3-MO domain with the enzyme installing hydroxyl at the bridgehead position of toralactone (**7**, Scheme 2b). The hydroxylated intermediate **24** would be far more susceptible to lactone hydrolysis due to the loss of conjugation and aromaticity and the favorable enolate leaving group. Hydrolysis—enzyme catalyzed or spontaneous—would result in acid **25**. Loss of carbon dioxide from acid **25** to generate the *o*-dihydroquinone **14** would likely be spontaneous and rapid with the re-establishment of aromaticity providing a large thermodynamic driving force. Alternatively, one could also consider a Baeyer–Villiger-like oxidation, with a flavin-C4a-peroxy nucleophile attacking the pyrone carbonyl. Ring expansion followed by hydrolysis and loss of carbon dioxide would generate the same product **14**. We consider this mechanism to be unlikely. The *p*-hydroxybenzoate monooxygenase enzyme family invariably proceeds through an electrophilic flavin-C4a-hydroperoxy species while flavoenzyme catalyzed Baeyer–Villiger oxidations rely on the nucleophilic flavin-C4a-peroxy species.[49]

There is precedence for *p*-hydroxybenzoate monooxygenase family members participating in oxidative aromatic ring cleavage. The enzymes 2-methyl-3-hydroxypyridine-5-carboxylic acid (MHPC, **26a**) oxygenase (MHPCO) and 5-pyridoxic acid (5PA, **26b**) oxygenase (5PAO) are flavoenzymes of the *p*-hydroxybenzoate monooxygenase family catalyzing aromatic hydroxylation and subsequent aromatic ring cleavage reactions (Scheme 2c).[50] Like conventional flavin monooxygenases, these enzymes use the flavin-C4a-hydroperoxy reactive intermediate (**21**) in their initial electrophilic aromatic oxidation; however,

DOI: 10.1021/jacs.6b00633
J. Am. Chem. Soc. 2016, 138, 4219–4228

they undergo a subsequent ring-opening reaction. The mechanism of ring opening has not been definitively established, but it is known that ring opening is enzyme catalyzed in MHPCO and involves the addition of water to the carbonyl intermediate (**27a**).[51]

The evolution of cercoquinones C and D and their putative shared intermediate **14** are in keeping with the proposed mechanism (Scheme 2b). The transfer of a hydride equivalent from dihydroquinone **14** to FAD_{ox}, while not anticipated, is not unreasonable. In the absence of a reductive environment, one could envision this oxidation is the dominant pathway toward cercoquinone C as we observe. Furthermore, the observed consumption of *nor*-toralactone by CTB3-MO implies an *ortho*-quinone intermediate. *Ortho*-quinone analogues of cercoquinone C have been used previously to access the perylenequinone core through simple coupling under acidic conditions.[52−54] Assuming *nor*-toralactone serves as an alternative substrate for CTB3-MO, the observed but uncharacterized dimeric products could likely arise through analogous couplings.

Under reductive conditions (DTT), cercoquinone C upon release would be rapidly reduced back to species **14**. Electron-rich naphthalene species such as compound **14** are highly prone to spontaneous oxidation. One could envision the oxidation of compound **14** to cercoquinone D as being rapid and complete, even under reductive conditions. The apparent instability of intermediate **14** could explain the observed preference for oxidation of *ortho*-quinone cercosporin C. In the quinone oxidation state, this species is protected from subsequent oxidation, ensuring biosynthetic fidelity.

Structural analysis of known fungal perylenequinone natural products reveals several common features among this family of metabolites (Figure 6).[54] First, the 7, 7′ moieties are derived from 2-oxypropyl side chains. Second, the 2, 2′ substituents are always methoxyl, or in the case of cercosporin a derivative thereof. Third, the 6, 6′ substituents are always methoxyl or derivatives thereof. Fourth, the perylenequinone core architecture remains unaltered. These core structural features suggest a common biosynthetic pathway for the perylenequinone metabolites. Indeed, the activities of CTB1, CTB3, CTB2, and CTB5 delineated here would account for each of these features with CTB1 producing the common intermediate *nor*-toralactone, CTB3 methylating this intermediate at the OH-2 and opening the pyrone ring thereby installing a C6-OH, CTB2 methylating the nascent C6-OH, and CTB5 catalyzing dimerization yielding the perylenequinone carbon core. Interestingly, homologues of each of these enzymes are found in known gene clusters most similar to the CTB cluster. Of these clusters, only one is linked to a known product, hypocrellin A (**13**).[35] Hypocrellin A differs from cercosporin in three key features: the 7, 7′ substituents are retained in the 2-oxypropyl oxidation state and are linked through an intramolecular aldol reaction, the 2, 2′ substituents are methoxyl, and the compound adopts the opposite atropisomeric configuration. Comparing the CTB and hypocrellin A biosynthetic clusters, CTB6 and CTB7 appear unique to the CTB cluster. Given that these enzymes presumptively reduce the 2-oxypropyl substituents and install the dioxepine moiety, respectively, it makes sense that they would be missing in the hypocrellin A cluster, where these structural features are not present. Altogether, these data imply that perylenequinone natural products proceed through a common biosynthetic pathway in which *nor*-toralactone is initially produced and further processed by a CTB3 didomain homologue. Given its unique coupled activities, CTB3 and its homologues make appealing targets for antifungal agents.

CONCLUSION

Here we resolve the long-standing ambiguity of cercosporin biosynthesis and propose an alternative biosynthetic pathway. We demonstrate that the naphthoquinone *nor*-toralactone is an essential intermediate of the cercosporin pathway, further corroborating the previously observed *in vitro* activity of the NR-PKS CTB1.[25] We also characterize the activity of the unusual didomain protein CTB3 showing that its flavin-dependent monooxygenase domain is responsible for an uncommon oxidative aromatic cleavage. Together, these findings further not only our understanding of perylenequinone biosynthesis but also expand the known biochemical repertoire of flavin-dependent monooxygenases—an important class of enzymes in both primary and secondary metabolism. While addressing in detail the initial steps of cercosporin biosynthesis, data presented only partially resolve the later portion of the biosynthetic pathway. The crucial perylenequinone dimerization step(s) and how the absolute configurations of the atropisomers are set remain intriguing, unanswered mechanistic questions. Given the importance of cercosporin and its congeners for plant pathogenicity, disruption of these steps or the rare confluence of CTB3 activities present opportunities for the development of selective antifungal agents against *Cercospora* species.

ASSOCIATED CONTENT

Supporting Information

The Supporting Information is available free of charge on the ACS Publications website at DOI: 10.1021/jacs.6b00633.

Experimental details, CTB3 and CTB2 sequence details, full results of complementation assay and CTB3 + CTB2 *in vitro* reactions, and compound spectra. (PDF)

AUTHOR INFORMATION

Corresponding Author

*ctownsend@jhu.edu

Notes

The authors declare no competing financial interest.

ACKNOWLEDGMENTS

We particularly thank Dr. Kuang-Ren Chung (National Chung Hsing University, Taichung, Taiwan) for providing *C. nicotianae* (ATCC 18366) wild type and CTB gene cluster knockout strains. We thank Philip A. Storm and Callie R. Huitt-Roehl (Department of Chemistry, Johns Hopkins University, Baltimore, MD, USA) for helpful conversations. The authors declare no financial conflicts of interest. This work was supported by NIH Grant ES001670.

REFERENCES

(1) Daub, M. E. *Phytopathology* **1981**, *71*, 213−213.
(2) Morgan, B. J.; Dey, S.; Johnson, S. W.; Kozlowski, M. C. *J. Am. Chem. Soc.* **2009**, *131*, 9413−9425.
(3) Morgan, B. J.; Mulrooney, C. A.; Kozlowski, M. C. *J. Org. Chem.* **2010**, *75*, 44−56.
(4) Daub, M. E.; Herrero, S.; Chung, K. R. *FEMS Microbiol. Lett.* **2005**, *252*, 197−206.
(5) Kuyama, S.; Tamura, T. *J. Am. Chem. Soc.* **1957**, *79*, 5725−5726.

DOI: 10.1021/jacs.6b00633
J. Am. Chem. Soc. 2016, 138, 4219−4228

(6) Kuyama, S.; Tamura, T. *J. Am. Chem. Soc.* **1957**, *79*, 5726−5729.
(7) Lousberg, R. J. J. C.; Weiss, U.; Salemink, C. A.; Arnone, A.; Merlini, L.; Nasini, G. *J. Chem. Soc. D* **1971**, 1463−1464.
(8) Yamazaki, S.; Ogawa, T. *Agric. Biol. Chem.* **1972**, *36*, 1707−1718.
(9) Nasini, G.; Merlini, L.; Andreetti, G. D.; Bocelli, G.; Sgarabotto, P. *Tetrahedron* **1982**, *38*, 2787−2796.
(10) Daub, M. E.; Hangarter, R. P. *Plant Physiol.* **1983**, *73*, 855−857.
(11) Dobrowolski, D. C.; Foote, C. S. *Angew. Chem., Int. Ed. Engl.* **1983**, *22*, 720−721.
(12) Daub, M. E. *Plant Physiol.* **1982**, *69*, 1361−1364.
(13) Daub, M. E.; Briggs, S. P. *Plant Physiol.* **1983**, *71*, 763−766.
(14) Daub, M. E.; Ehrenshaft, M. *Annu. Rev. Phytopathol.* **2000**, *38*, 461−490.
(15) Yamazaki, S.; Okubo, A.; Akiyama, Y.; Fuwa, K. *Agric. Biol. Chem.* **1975**, *39*, 287−288.
(16) Fajola, A. O. *Physiol. Plant Pathol.* **1978**, *13*, 157−164.
(17) Daub, M. E. *Phytopathology* **1982**, *72*, 370−374.
(18) Choquer, M.; Dekkers, K. L.; Chen, H. Q.; Cao, L. H.; Ueng, P. P.; Daub, M. E.; Chung, K. R. *Mol. Plant-Microbe Interact.* **2005**, *18*, 468−476.
(19) Choquer, M.; Lee, M. H.; Bau, H. J.; Chung, K. R. *FEBS Lett.* **2007**, *581*, 489−494.
(20) Dekkers, K. L.; You, B. J.; Gowda, V. S.; Liao, H. L.; Lee, M. H.; Bau, H. H.; Ueng, P. P.; Chung, K. R. *Fungal Genet. Biol.* **2007**, *44*, 444−454.
(21) Daub, M. E.; Leisman, G. B.; Clark, R. A.; Bowden, E. F. *Proc. Natl. Acad. Sci. U. S. A.* **1992**, *89*, 9588−9592.
(22) Leisman, G. B.; Daub, M. E. *Photochem. Photobiol.* **1992**, *55*, 373−379.
(23) Sollod, C. C.; Jenns, A. E.; Daub, M. E. *Appl. Environ. Microbiol.* **1992**, *58*, 444−449.
(24) Okubo, A.; Yamazaki, S.; Fuwa, K. *Agric. Biol. Chem.* **1975**, *39*, 1173−1175.
(25) Newman, A. G.; Vagstad, A. L.; Belecki, K.; Scheerer, J. R.; Townsend, C. A. *Chem. Commun.* **2012**, *48*, 11772−11774.
(26) Chen, H. Q.; Lee, M. H.; Daub, M. E.; Chung, K. R. *Mol. Microbiol.* **2007**, *64*, 755−770.
(27) Chen, H. Q.; Lee, M. H.; Chung, K. R. *Microbiology* **2007**, *153*, 2781−2790.
(28) Chung, K. R.; Jenns, A. E.; Ehrenshaft, M.; Daub, M. E. *Mol. Gen. Genet.* **1999**, *262*, 382−389.
(29) Chung, K. R.; Daub, M. E.; Kuchler, K.; Schuller, C. *Biochem. Biophys. Res. Commun.* **2003**, *302*, 302−310.
(30) Herrero, S.; Amnuaykanjanasin, A.; Daub, M. E. *FEMS Microbiol. Lett.* **2007**, *275*, 326−337.
(31) Akache, B.; Wu, K.; Turcotte, B. *Nucleic Acids Res.* **2001**, *29*, 2181−2190.
(32) Ehrenshaft, M.; Upchurch, R. G. *Appl. Environ. Microbiol.* **1991**, *57*, 2671−2676.
(33) Jenns, A. E.; Daub, M. E. *Phytopathology* **1996**, *85*, 906−912.
(34) Weber, T.; Blin, K.; Duddela, S.; Krug, D.; Kim, H. U.; Bruccoleri, R.; Lee, S. Y.; Fischbach, M. A.; Muller, R.; Wohlleben, W.; Breitling, R.; Takano, E.; Medema, M. H. *Nucleic Acids Res.* **2015**, *43*, W237−243.
(35) Yang, H.; Wang, Y.; Zhang, Z.; Yan, R.; Zhu, D. *Genome Announce.* **2014**, *2*, e00011−14.
(36) Ebnother, A.; Meijer, T. M.; Schmid, H. *Helv. Chim. Acta* **1952**, *35*, 910−928.
(37) Vessecchi, R.; Emery, F. S.; Lopes, N. P.; Galembeck, S. E. *Rapid Commun. Mass Spectrom.* **2013**, *27*, 816−824.
(38) Vessecchi, R.; Emery, F. S.; Galembeck, S. E.; Lopes, N. P. *Rapid Commun. Mass Spectrom.* **2010**, *24*, 2101−2108.
(39) Vessecchi, R.; Emery, F. S.; Galembeck, S. E.; Lopes, N. P. *J. Mass Spectrom.* **2012**, *47*, 1648−1659.
(40) Wheeler, M. H.; Klich, M. A. *Pestic. Biochem. Physiol.* **1995**, *52*, 125−136.
(41) Bauer, W.; Zenk, M. H. *Tetrahedron Lett.* **1989**, *30*, 5257−5260.
(42) Rueffer, M.; Zenk, M. H. *Phytochemistry* **1994**, *36*, 1219−1223.
(43) Medentsev, A. G.; Akimenko, V. K. *Phytochemistry* **1998**, *47*, 935−959.
(44) Eisenman, H. C.; Casadevall, A. *Appl. Microbiol. Biotechnol.* **2012**, *93*, 931−940.
(45) Chen, Z.; Nunes, M. A.; Silva, M. C.; Rodrigues, C. J., Jr. *Mycologia* **2004**, *96*, 1199−1208.
(46) Thomas, P. W.; Stone, E. M.; Costello, A. L.; Tierney, D. L.; Fast, W. *Biochemistry* **2005**, *44*, 7559−7569.
(47) Huijbers, M. M. E.; Montersino, S.; Westphal, A. H.; Tischler, D.; van Berkel, W. J. H. *Arch. Biochem. Biophys.* **2014**, *544*, 2−17.
(48) Entsch, B.; van Berkel, W. J. *FASEB J.* **1995**, *9*, 476−483.
(49) Mirza, I. A.; Yachnin, B. J.; Wang, S.; Grosse, S.; Bergeron, H.; Imura, A.; Iwaki, H.; Hasegawa, Y.; Lau, P. C.; Berghuis, A. M. *J. Am. Chem. Soc.* **2009**, *131*, 8848−8854.
(50) Chaiyen, P. *Arch. Biochem. Biophys.* **2010**, *493*, 62−70.
(51) Chaiyen, P.; Brissette, P.; Ballou, D. P.; Massey, V. *Biochemistry* **1997**, *36*, 8060−8070.
(52) Hauser, F. M.; Sengupta, D.; Corlett, S. A. *J. Org. Chem.* **1994**, *59*, 1967−1969.
(53) Merlic, C. A.; Aldrich, C. C.; Albaneze-Walker, J.; Saghatelian, A.; Mammen, J. *J. Org. Chem.* **2001**, *66*, 1297−1309.
(54) Mulrooney, C. A.; Morgan, B. J.; Li, X.; Kozlowski, M. C. *J. Org. Chem.* **2010**, *75*, 16−29.

DOI: 10.1021/jacs.6b00633
J. Am. Chem. Soc. 2016, 138, 4219−4228